Biomolecules and Biomedicine

ISSN: 2831-0896 (Print) | ISSN: 2831-090X (Online)

Journal Impact Factor® (2023): 3.1

CiteScore® (2023): 7.4

www.biomolbiomed.com | www.blog.bjbms.org

RESEARCH ARTICLE

Wen et al: CACYBP knockdown inhibits LUAD progression

Silencing CACYBP suppresses lung adenocarcinoma growth via CDK1 inhibition

Ge Wen[1,2], Shaoqing Niu[3], Shiqi Mei[4] and Senming Wang[1*]

[1]Department of Oncology, Zhujiang Hospital, Southern Medical University, Guangzhou, China

[2]Department of Radiation Oncology; Guangdong Provincial Key Laboratory of Major Obstetric Diseases; Guangdong Provincial Clinical Research Center for Obstetrics and Gynecology; The Third Affiliated Hospital, Guangzhou Medical University, Guangzhou, China

[3]Department of Radiation Oncology, First Affiliated Hospital of Sun Yat-sen University, Guangzhou, China

[4]Department of Oncology, The Second School of Clinical Medicine, Southern Medical University, Guangzhou, China

[*]**Correspondence to** Senming Wang: wsm@smu.edu.cn.

DOI: https://doi.org/10.17305/bb.2025.11849

ABSTRACT

Calcyclin-binding protein (CACYBP) is a multidomain adaptor protein implicated in the development of various cancers. However, its molecular and biological roles in lung adenocarcinoma (LUAD) remain unclear. In this study, we aimed to elucidate the biological impact of CACYBP in LUAD. Immunohistochemistry was used to assess CACYBP expression in LUAD tissues. Lentivirus-mediated CACYBP knockdown was established in LUAD cell lines, and target gene expression was analyzed via Western blotting and qRT-PCR. Cell proliferation, apoptosis, and migration were evaluated using flow cytometry, colony formation assays, Cell Counting Kit-8 (CCK-8 assays), Celigo cell counting, wound healing assays, Transwell assays, and mouse xenograft models. Co-immunoprecipitation was performed to verify the interaction between CACYBP and Cyclin-dependent kinase 1 (CDK1). Additionally, the Phosphoinositide 3-kinase (PI3K) inhibitor LY294002 was used to investigate the involvement of CDK1 in the PI3K/AKT pathway. Our findings revealed that CACYBP was upregulated in LUAD tissues and correlated with advanced disease stages and poor prognosis. CACYBP knockdown inhibited LUAD progression and metastasis, promoted cell apoptosis *in vitro*, and reduced tumorigenicity *in vivo*. Mechanistically, we identified CDK1 as a direct interacting partner of CACYBP. CDK1 overexpression enhanced the malignant phenotype of LUAD cells and partially reversed the inhibitory effects of CACYBP knockdown. Furthermore, inhibition of the PI3K/AKT pathway using LY294002 significantly suppressed CDK1-mediated LUAD cell growth. In conclusion, CACYBP appears to function as a tumor promoter in LUAD, at least in part through CDK1-mediated activation of the PI3K/AKT pathway. These findings suggest that CACYBP could serve as a promising therapeutic target and a novel biomarker for LUAD prognosis.

Keywords: Calcyclin-binding protein; CACYBP; lung adenocarcinoma; LUAD; cyclin-dependent kinase 1; CDK1; PI3K/AKT pathway; proliferation.

INTRODUCTION

Lung cancer has the highest incidence and mort ality rates among cancers globally, and non-small cell lung cancer (NSCLC) accounts for 80% to 85% of all lung cancer cases worldwide [1, 2]. In addition, lung adenocarcinoma (LUAD) has the highest prevalence among the histological subtypes of NSCLC [3]. LUAD is asymptomatic in the early stage and is prone to metastasis and recurrence. At the time of preliminary diagnosis, most patients have already reached the advanced stage, which contributes to the high rate of cancer-related death [4, 5]. Although the development of targeted therapy and immunotherapy in combination with standard therapies has improved the clinical outcomes of LUAD patients, an unsatisfactory prognosis occurs due to low response rates to immunotherapeutic agents in a certain number of patients and inevitable resistance to targeted drugs [6-8]. Therefore, determining the potential mechanisms regulating LUAD development and its progress for identifying promising therapeutic targets and improving the prognosis of LUAD is crucial.

A multidomain calcyclin binding protein (CACYBP) can interact with the S100 family, Siah-1, Skp1, Tubulin, ERK1/2, and Nrdp1 through different binding sites and participate in several cellular processes, such as the ubiquitination of proteins, rearrangement of the cytoskeleton, proliferation, differentiation, and autophagy of cells, and regulation of the cell cycle [9-12]. Previous studies have shown that CACYBP has different functions in the development of various tumors. For example, CACYBP could become a tumor promoter in cholangiocarcinoma, liver and prostate cancers [13-15]. In contrast, CACYBP may be a negative regulator of cell proliferation in astrocytoma and renal cell carcinoma [16, 17]. In addition, CACYBP could become a tumor suppressor during breast cancer [18]. Another study indicated that CACYBP is a tumor promoter of breast carcinogenesis [19]. Therefore, CACYBP regulates tumor growth and advancement; however, specific profiles of CACYBP expression in different tumors may be heterogeneous.

Recently, key genes associated with sphingomyelin metabolic activity, including CACYBP, have been screened by integrating single-cell RNA-seq and bulk RNA-seq data, and a LUAD prognostic prediction model has been established [20]. Nevertheless, the exact function and specific molecular mechanism of CACYBP in LUAD remain to be elucidated. Thus, in this study, the biological process of CACYBP in LUAD cells was evaluated by knocking down CACYBP and exploring the regulatory mechanisms involved.

MATERIALS AND METHODS

TCGA database analysis

The RNA-seq raw counts and clinical data of LUAD were downloaded from The Cancer Genome Atlas (TCGA) database through the Genomic Data Commons (GDC) data portal (https://portal.gdc.cancer.gov/) using the GDC-client and were then preprocessed using the R/Bioconductor software package "TCGAbiolinks" [21]. A total of 524 tumor tissue samples and 59 normal tissue samples were available, which included 57 paired samples. Subsequently, the expression data were standardized, and the differentially expressed genes (DEGs) between LUAD and normal tissues were analyzed using the R/Bioconductor software package "DESeq2", where an absolute fold change ≥ 1.5, $p < 0.05$ and a false discovery rate (FDR) < 0.05 were set as the thresholds for screening DEGs [22].

Immunohistochemistry (IHC) of clinical specimens

Paraffin-embedded specimens from 96 LUAD tissues and 87 adjacent noncancerous tissues were obtained along with clinicopathologic information from The Third Affiliated Hospital of Guangzhou Medical University, and the Ethics Committee approved the study design. After xylene deparaffinization and rehydration in a graded alcohol series, we boiled the sections using citrate buffer in an autoclave. Then, they were blocked sequentially with 3% H_2O_2 and goat serum before overnight incubation at 4 ℃ using primary anti-CACYBP (1:100, ab171972, Abcam), anti-CDK1 (1:100, HPA003387, Sigma) or anti-Ki-67 (1:200, ab16667, Abcam). After washing, sequential incubation of the sections was performed using HRP-conjugated goat anti-rabbit secondary antibody (1:400, ab6721, Abcam) and DAB, followed by hematoxylin counterstaining. Then, we obtained images using an inverted microscope and assessed them based on staining intensity and percentage [23]. The proportion score was multiplied by the intensity score to yield an immunoreactivity score that ranged from 0 to 12. A score of 0 – 4 was considered to indicate low CACYBP expression, and a score of 5 – 12 was considered to indicate high CACYBP expression.

Cell lines and culture conditions

For the downstream analysis, BEAS-2B, a line of normal human bronchial epithelial cells, was obtained from Cobioer (Nanjing, China). The human LUAD cell lines A549 and NCI-H1299 and the lung squamous cell carcinoma cell line EBC-1 were obtained from the China Center for Type Culture Collection. Cells were grown in DMEM (Gibco; Thermo Fisher Scientific, Inc., Waltham, MA, USA) (BEAS-2B), Ham's F-12K (Gibco; A549), RPMI-1640

(Gibco; NCI-H1299), or MEM (Gibco; EBC-1), with 10% FBS added to these media. The reactions were carried out in a 37 °C, 5% CO_2 incubator with constant humidity.

Plasmid construction and lentivirus preparation

Shanghai Bioscienceres Co., Ltd. (Shanghai, China) helped construct all lentiviral vectors and helper plasmids. Interfering lentiviral vectors were constructed by inserting three short hairpin RNA (shRNA) sequences targeting CACYBP into the BR-V108 plasmid. The shCACYBP target sequences were shCACYBP-1, 5′ – AGCCAAAGGAGACACGGAATT – 3′; shCACYBP-2, 5′ – ATGATATGAAGCGAACCATTA – 3′; and shCACYBP-3, 5′ – GAATCTAAATGGGAAGAGTTA – 3′. In addition, we developed CDK1-overexpressing cells by cloning the CDK1 coding sequence within the LV013 plasmid. Cells transfected with corresponding empty plasmids served as negative controls (shCtrl). Positive transfection was determined by detecting green fluorescence under a fluorescence microscope.

Quantitative reverse transcription polymerase chain reaction (qRT–PCR)

TRIzol Reagent (Sigma, Beijing, China) was used to extract total RNA from cultured cells. Then, the HiScript Q RT SuperMix for qPCR (+gDNA wiper) Kit (Vazyme, Nanjing, China) helped reverse-transcribe into complementary DNA following the protocols of the product kit. Subsequently, qRT–PCR was conducted based on the guidelines of the AceQ qPCR SYBR Green Master Mix Kit (Q111-02, Vazyme, Nanjing, China). After normalization against the internal reference gene GAPDH, the $2^{-\Delta\Delta Ct}$ method was used to quantify the mRNA levels. Sangon Biotech (Shanghai, China) developed the primers for qRT–PCR. Table S1 provides the list of the involved sequences.

Western blotting and co-immunoprecipitation (co-IP) assays

RIPA lysis buffer (Beyotime Biotechnology, Shanghai, China) facilitated total protein collection from the cultured cells. The BCA Protein Assay Kit (Pierce; Thermo Fisher Scientific, Inc.) assessed the protein concentrations. The protein preparation (20 μg) underwent separation using 10% SDS–PAGE (Beyotime Biotechnology) and transferred to a PVDF membrane. TBST solution (5% skimmed milk) helped block the membranes at room temperature for 1 h, followed by incubation with primary antibody at 4 ℃ overnight and secondary antibody for an additional 2 h. Immunoreactivity was assessed via the enhanced chemiluminescence (ECL) method based on the Immobilon Western Chemiluminescent HRP Substrate Kit (Millipore; Merck KGaA).

For co-IP, the protein (1.0 mg) was incubated first with diluted antibodies at 4 ℃ overnight and then incubated for an additional 2 h with magnetic beads (20 μL). After centrifugation, IP lysis buffer was used to wash the obtained pellet. Then, the complexes were denatured in IP lysis and 5 × loading buffers using boiling water at 100 ℃ for 5 min. The resulting reactants were analyzed by western blotting. The western blotting and co-IP antibodies are presented in Table S2.

Cell Counting Kit-8 (CCK-8) assay

A549 and NCI-H1299 cells were seeded into 96-well plates (2,500 cells/100 μL/well) in the logarithmic growth phase and subjected to various treatments or transfections. They were cultured at 37 ℃ in 5% CO_2. From the second day after plating, 10 μL of CCK-8 reagent (Sigma; Merck KGaA) was added to the wells before culture termination. After an additional 2 h incubation, the optical density was calculated for each well at 450 nm with a Tecan Infinite 200 Pro microplate reader.

Colony formation assay

The colony formation was examined using cultured lentivirus-transfected A549 and NCI-H1299 cells in six-well plates (1,000 cells/2 mL/well). The cells were incubated for 8 days with the medium refreshed every 3 days. After 4% paraformaldehyde fixation and Giemsa staining, counting and analyzing colonies in the control and experimental groups was performed.

Celigo cell counting assay

A549 and NCI-H1299 cells were seeded into 96-well plates (2,000 cells/100 μL/well). Only the logarithmic growth phase cells subjected to various treatments or transfections were seeded, followed by overnight 5% CO_2 incubation at 37 ℃. Cell numbers were monitored daily, and proliferation curves were developed for five consecutive days starting on day 2 with a Celigo image cytometer (Nexcelom Bioscience, Lawrence, MA, USA).

Flow cytometry analysis of apoptosis

The cell apoptosis was examined using cultured lentivirus-transfected A549 and NCI-H1299 cells in six-well plates (8×10^5 cells/2 mL/well). After 96 hours, we obtained and stained the cultured cells for the cell apoptosis assays using the Annexin V-allophycocyanin (APC) Apoptosis Detection Kit (Invitrogen; Thermo Fisher Scientific, Inc.) following the kit's instructions. Apoptosis was analyzed with flow cytometry (Guava easyCyte HT, Millipore; Merck KGaA).

Migration assays

Wound healing and Transwell assays were used to evaluate the ability of lentivirus-transfected A549 and NCI-H1299 cells to migrate.

Transfected cells (5×10^4 cells/well) were grown in 96-well plates to form a confluent monolayer for evaluating wound healing. Wounds were generated in the monolayers with a 96-wounding replicator (V&P Scientific). After gently rinsing the monolayers thrice with serum-free medium, 0.5% FBS was introduced within the wells for culture. Subsequently, the migration progress was photographed post-scratching at 0 h and appropriate time points. ImageJ software was used to calculate the distance between the advancing cell edges.

We used 24-well Transwell inserts (8-μm pore size, Corning) for the assays. The transfected cells (5×10^4 cells/well) were resuspended in 100 μL of serum-free medium and plated within the upper chamber. We added medium (600 μL) containing 30% FBS inside the lower chamber. After 30 h or 48 h of growth, non-migrated cells were gently removed with a cotton swab. After 4% paraformaldehyde fixation and Giemsa staining, the migrated cells were photographed under an inverted microscope (IX73, Olympus) and randomly counted in five fields.

Mouse xenograft model

The animal experiments received approval from the Third Affiliated Hospital of Guangzhou Medical University (Approval No. S2021-120). All experimental procedures adhered to the Guidelines for the Ethical Review of Laboratory Animal Welfare, China (GB/T 35892-2018) [24]. A cohort of 20 female BALB/c nude mice, aged four weeks, was procured from Beijing Vital River Laboratory Animal Technology Co., Ltd. (Beijing, China). Prior to the initiation of any experimental procedures, the mice were allowed to acclimatize to the laboratory environment. The mice were housed in groups of five per standard cage within an independent ventilated cage system, which maintained controlled conditions of temperature (22 – 24 ℃), humidity (50 – 60%), and a 12-hour light/dark cycle. High-quality corncob bedding was provided and replaced biweekly. The mice had ad libitum access to standard laboratory rodent chow and sterilized water, with water changes occurring weekly. All procedures were conducted under anesthesia, with rigorous efforts made to minimize animal distress and suffering.

Mice were randomly allocated into two groups, shCACYBP and shCtrl, with each group comprising 10 mice. To establish mouse xenograft models, transfected NCI-H1299 cells (4×10^6 cells, suspended in 200 μL of PBS) were subcutaneously injected into the right axilla of

the mice. Tumor diameter and body weight were measured weekly, and tumor volume was calculated using the formula $\pi/6 \times \text{length} \times \text{width}^2$. Predefined humane endpoints were set at a tumor volume of ≤ 2,000 mm³ or a weight loss of ≥ 20%, and no mice reached these thresholds during the study. On day 35 post-injection, *in vivo* fluorescence imaging of the tumors was conducted using the IVIS Spectrum In Vivo Imaging System (PerkinElmer, Waltham, MA, USA). Following imaging, the mice were euthanized, and the excised tumor tissues were weighed and stored at −80 ℃ for further analysis.

RNA screening analysis

Gene expression profiling and RNA screening analysis of NCI-H1299 cells transfected with shCACYBP or shCtrl were conducted by Shanghai Biosciencereces Co., Ltd. (Shanghai, China). The TRIzol method was used to extract the total RNA, which was quantified using a Nanodrop 2000 system (Thermo Fisher Scientific, Inc.). The Human Clariom S assay (Affymetrix, Thermo Fisher Scientific, Inc.) was used to explore the gene expression profile following the kit's protocols. After scanning and analyzing the cartridge arrays with a GeneChip® Scanner 3000 7G System (Affymetrix, Thermo Fisher Scientific, Inc.), we identified the DEGs in NCI-H1299-shCACYBP and NCI-H1299-shCtrl cells with absolute fold change ≥ 1.5 and FDR < 0.05 thresholds. Ingenuity Pathway Analysis software (IPA, Ingenuity Systems, Qiagen Inc.) helped perform the enriched functional annotation and pathway analyses based on all DEGs, and absolute Z scores > 2 were considered to indicate significance.

Ethical statement

This study design was approved by the Research Ethics Committee of the Third Affiliated Hospital of Guangzhou Medical University (Approval No. S2021-120) in accordance with the Declaration of Helsinki and institutional guidelines.

Statistical analysis

Each experiment was performed separately at least three times. Data are represented as the mean and standard deviation (SD). SPSS 26.0 and GraphPad Prism 9.0 were used for data analysis. Moreover, Student's *t* test, Chi-square, and analysis of variance (ANOVA) were used for comparisons of obtained data as where applicable. Survival analysis was performed using the Kaplan–Meier method with the log-rank test. Statistical significance was principally determined by a two-tailed $p < 0.05$. RNA-seq analysis was conducted utilizing the R/Bioconductor software package "DESeq2", which employs a negative binomial generalized linear model to identify DEGs [22]. To address the issue of multiple comparisons inherent in

RNA-seq data, the $p < 0.05$ threshold was adjusted using the FDR control. Thresholds for significant DEGs were established at an absolute fold change ≥ 1.5 and a FDR < 0.05, in accordance with the Benjamini-Hochberg procedure for multiple testing correction [25].

RESULTS

CACYBP was up-regulated in LUAD and correlated with poor prognosis

Through the analysis of RNA-seq counts data of TCGA-LUAD cohort samples, it was found that the CACYBP (ENSG00000116161) gene was significantly up-regulated in tumor samples relative to normal tissues ($\log_2$FC = 0.862, $p = 3.99\times10^{-24}$). CACYBP gene expression levels in tumor samples were compared with those in normal tissues using the *t* test. The results of the comparative analysis of the population samples and 57 paired samples showed that the expression level of CACYBP mRNA in tumor tissues was significantly higher than that in normal tissues (Figure 1A and 1B, $p < 0.0001$).

Among 524 patients with LUAD, only 490 patients had complete clinical information with a median age of 65 years (range, 33 – 88 years), and these individuals were divided into low-expression and high-expression groups based on the median CACYBP gene expression levels in tumor samples. According to the chi-square test, there was a higher proportion of male patients in the high-expression group. In addition, the expression of CACYBP was associated with the TNM stages of LUAD patients (Table 1).

Furthermore, Kaplan–Meier survival analysis showed that the prognosis in terms of overall survival was worse in patients with high expression of CACYBP than in those with low expression of CACYBP ($p = 0.005$, Figure 1C). Therefore, these findings suggested that CACYBP may be involved in the occurrence, development, and prognosis of LUAD.

To validate the above bioinformatic prediction results, IHC tissue microarrays were used to detect the expression of the CACYBP protein in 96 LUAD tissues and 87 paired adjacent noncancerous tissues. CACYBP expression was found to be substantially greater in the cytoplasm of LUAD tissues (44/96, 45.8%) than in normal tissues (8/87, 9.2%; $p < 0.001$) (Figure 1D). Furthermore, CACYBP expression was up-regulated in tumor tissues in ten paired LUAD samples (Figure 1E).

According to the IHC results, 96 LUAD patients with a median age of 62 years (range, 34 – 87 years) were divided into two groups: a low CACYBP expression group (n = 52) and a high CACYBP expression group (n = 44). The relationship between CACYBP expression and the

clinicopathological characteristics of LUAD patients was further analyzed. The results showed that abnormal expression of CACYBP was closely related to TNM stages in LUAD patients (Table 2).

As of September 18, 2023, 72 patients (75.0%) had valid follow-up information. The median survival time was 19.5 months for the 39 patients in the low expression group and 13.6 months for the 33 patients in the high expression group. Kaplan–Meier survival analysis indicated that high CACYBP expression was associated with poor overall survival of LUAD patients (p = 0.010, Figure 1F). Our results further confirmed the bioinformatic predictions.

Construction of CACYBP knockdown lung cancer cell lines

Given the correlation of CACYBP with prognosis and clinicopathologic features, we attempted to explore the potential impact of CACYBP on the malignant biological phenotype of LUAD cell lines. CACYBP expression was confirmed to be higher in human NSCLC cell lines (NCI-H1299, A549, and EBC-1) than in the BEAS-2B cell line (normal bronchial epithelial cells) (Figure 2A and 2B). Subsequently, three shRNAs were designed and synthesized to knock down CACYBP in NCI-H1299 cells. Based on qRT–PCR analysis, CACYBP relative mRNA levels were lowered by 85.0% in the shCACYBP-1 group and 88.3% in the shCACYBP-2 group but not in the shCACYBP-3 group (Figure 2C). To avoid off-target effects, two independent shRNAs (shCACYBP-1 and shCACYBP-2) were used to generate tagged stable cell lines.

After 72 hours of lentivirus-mediated transfection, shCACYBP-1 and shCACYBP-2 significantly inhibited the expression of CACYBP mRNA and protein in A549 and NCI-H1299 cell lines (Figure 2D and 2E). Thus, these cells could be used for subsequent cellular function assays.

CACYBP knockdown inhibits progression-related processes in LUAD cells *in vitro*

CCK-8 and colony formation assays demonstrated that CACYBP silencing led to significant inhibition of A549 and NCI-H1299 cell proliferation (Figure 3A and 3B). Moreover, the flow cytometry results showed that CACYBP silencing could lead to apoptosis in A549 and NCI-H1299 cells (Figure 3C). Subsequently, the effect of CACYBP knockdown on migration was evaluated using wound healing and Transwell assays and showed that A549 and NCI-H1299 cell migration was significantly inhibited (Figure 3D and 3E). Therefore, these *in vitro* experiments demonstrated that CACYBP down-regulation inhibited LUAD cell proliferation

and migration, enhancing apoptosis. We chose shCACYBP-2 for further experiments due to its higher knockdown efficiency.

CACYBP knockdown inhibits LUAD tumor growth *in vivo*

The CACYBP knockdown effect on LUAD proliferation was validated *in vivo* by developing mouse xenograft models through subcutaneous injection of transfected NCI-H1299 cells using shCACYBP-2 or shCtrl. Tumor fluorescence intensity was drastically reduced in the shCACYBP group compared to the shCtrl group (Figure 4A and 4B). The shCACYBP group had significantly lower tumor number, volume, and weight (according to analysis of samples obtained by tumor resection) than the shCtrl group (Figure 4C–4E). Furthermore, IHC staining revealed decreased expression of the nuclear proliferation antigen Ki-67 in the shCACYBP group (Figure 4F). Overall, these results indicate that LUAD proliferation is inhibited by CACYBP knockdown *in vivo*.

CACYBP depletion inhibited LUAD progression via CDK1

RNA-seq was performed to identify DEGs in NCI-H1299 cells transfected with shCACYBP or shCtrl. Approximately 1823 DEGs were detected: 731 were up-regulated, and 1092 were down-regulated in shCACYBP cells compared to shCtrl cells (Figure 5A). Subsequently, IPA was used to evaluate DEG enrichment in canonical signaling pathways (Figure S1A) and diseases and functions (Figure S1B). Canonical pathway analysis revealed significant inhibition of several cancer-related pathways, including ERK/MAPK, PI3K/AKT, and CXCR4 signaling pathways (Figure S1A). The most notable enrichment of DEGs was observed within the "cancer" and "organismal injury and abnormalities" categories (Figure S1B). Interaction network analysis based on the enrichment results of all DEGs demonstrated that CACYBP could indirectly affect downstream genes in the ERK/MAPK signaling, PI3K/AKT signaling, CXCR4 signaling, and cyclin and cell cycle regulation pathways (Figure 5B).

Based on the interaction network, 20 down-regulated downstream genes were chosen for qRT–PCR verification. In addition, Western blotting confirmed four of these results. The results showed that the shCACYBP group had reduced CDK1, CCND1, and PLK1 mRNA and protein expression levels, while those of EGR1 were not (Figure 5C and 5D). Among these proteins, CDK1 is a potent cell cycle regulator and was assumed to be a promising target candidate for CACYBP.

IHC staining and co-IP assay were performed to validate this hypothesis: there was significantly higher CDK1 protein expression in LUAD tissues than in adjacent normal tissues

(Figure 5E), and the co-IP assay demonstrated a CACYBP and CDK1 protein interaction (Figure 5F). These results indicated that CDK1 expression in LUAD showed a similar pattern to CACYBP expression. Therefore, CDK1 was considered a downstream CACYBP target involved in NCI-H1299 cell regulation and was further validated by *in vitro* experiments.

CDK1 overexpression rescued CACYBP knockdown-mediated inhibition of LUAD

Rescue assays were used to determine the synergistic functions of CDK1 and CACYBP in developing LUAD. CDK1 mRNA expression was confirmed to be higher in NCI-H1299, A549, and EBC-1 cells by qRT–PCR than in BEAS-2B cells (Figure S2A). Therefore, NCI-H1299 cell models with CDK1 overexpression only (CDK1+NC (KD)), CACYBP knockdown only (shCACYBP+NC (OE)), simultaneous CDK1 overexpression and CACYBP knockdown (CDK1+shCACYBP) and negative control (NC (OE+KD)) were constructed (Figure 6A, 6B and S2B). Functional experiments indicated that CDK1 overexpression enhanced proliferation (Figure 6C and S2C) and migration (Figure 6E and 6F) and inhibited apoptosis (Figure 6D) of NCI-H1299 cells. Furthermore, CDK1 up-regulation partially reversed CACYBP knockdown-induced proliferation and migration inhibition and apoptosis elevation in NCI-H1299 cells (Figure 6C–6F and S2C). Thus, rescue experiments demonstrated that the effect of CACYBP on LUAD growth may be mediated by CDK1.

CDK1 promotes the growth of LUAD cells in a PI3K/AKT pathway-dependent manner

We explored whether the CDK1 effect on LUAD cells depended on the PI3K/AKT pathway, which shCACYBP inhibited based on IPA. Rescue experiments were performed using the PI3K inhibitor LY294002 to assess A549 and NCI-H1299 cell proliferation and apoptosis. LY294002 treatment attenuated the effects of CDK1 on promoting proliferation and inhibiting apoptosis in A549 and NCI-H1299 cells (Figure 7A–7D). Therefore, CDK1 affects LUAD cell growth via the PI3K/AKT pathway.

DISCUSSION

CACYBP is differentially expressed in human tissues, showing high expression in the brain, heart, and esophagus and no or low expression in other normal tissues, but is aberrantly expressed in most tumor tissues [26]. Chen et al. reported that in pancreatic cancer, high CACYBP expression is significantly associated with poor differentiation, an advanced TNM clinical stage or distant metastasis [27]. Lian et al. found that patients with high CACYBP expression in hepatocellular carcinoma presented significantly decreased overall and disease-free survival [15]. Based on the TCGA dataset, we found that the expression of CACYBP

mRNA was significantly up-regulated in LUAD clinical samples relative to normal lung tissues and was correlated with the tumor stage and that patients with high CACYBP expression showed worse survival outcomes. These results suggest that CACYBP may be associated with the malignant phenotype of tumors.

In the present study, IHC was employed to detect CACYBP expression in clinical samples from LUAD patients. We found that the expression of the CACYBP protein was significantly higher in LUAD tissues than in adjacent noncancerous tissues. Positive CACYBP expression in LUAD was located in the cytoplasm and was correlated with an advanced clinicopathological stage but not with age, sex, tumor size or pathological grade. In addition, an association between high CACYBP expression and poor prognosis in LUAD patients was observed. These results suggest that CACYBP may act as a tumor promoter in LUAD, but the role of CACYBP in the tumorigenesis and progression of LUAD has rarely been reported and has not been fully elucidated.

CACYBP, as a multi-ligand protein, exhibited tissue-specific expression profiles and context-dependent roles in tumorigenesis. Comprehensive pan-cancer analysis has identified that CACYBP was up-regulated in 14 cancers, including lung, liver, colon, and pancreatic cancers as well as cholangiocarcinoma, while it was down-regulated in six cancers, such as kidney renal clear cell and prostate cancers, highlighting its dual functionality as an oncogene or tumor suppressor depending on the cancer type [28]. For instance, in liver cancer, CACYBP facilitated cell progression by modulating $p27^{Kip1}$ and cyclins [15], whereas its knockdown in prostate cancer impeded cancer progression by up-regulating p53 [14], suggesting an oncogenic function. Additionally, CACYBP knockdown inhibited pancreatic cancer cell growth by blocking the G1 to S phase transition, mediated by the down-regulation of Cyclin E, Cyclin A, and CDK2, alongside the up-regulation of $p27^{Kip1}$ and Rb [29]. It also enhanced colon cancer proliferation by interacting with Skp1 to degrade $p27^{Kip1}$ [30], and promoted cholangiocarcinoma progression by inhibiting MCM2 ubiquitination and then activating the Wnt/β-catenin signaling pathway [13]. In contrast, in astrocytoma patients, CACYBP expression was associated with a favorable prognosis, suggesting a tumor-suppressive function [16]. In renal cancer, CACYBP overexpression reduced Cyclin D1 by degrading β-catenin, thereby inhibiting cell growth and tumorigenicity, further supporting its tumor-suppressive role [17]. Notably, the role of CACYBP in gastric cancer, glioma, and breast cancer is controversial. In gastric cancer, CACYBP has been implicated in promoting cell proliferation by binding to Skp1, degrading $p27^{Kip1}$, and increasing Cyclin E [31, 32]. Conversely, it could also inhibit

gastric cancer cell proliferation by degrading β-catenin and dephosphorylating ERK1/2 [33, 34]. In glioma, CACYBP enhanced proliferation and reduces apoptosis by down-regulating p53 and p21, while increasing the activity of Akt, β-catenin, and ERK1/2, suggesting an oncogenic role [35, 36]. Nonetheless, it may also inhibit glioma cell migration and invasion via Siah1-mediated $p27^{Kip1}$ down-regulation in the cytoplasm [37]. In breast cancer, CACYBP knockdown increased proliferation and invasion by up-regulating COX-2 [18], although other studies proposed that CACYBP expression facilitated the clinical progression of breast cancer [38]. The observed discrepancies in the role of CACYBP across various cancer types may be attributed to the specific cellular context and the presence of distinct molecular pathways [28].

In this study, the findings demonstrated that the knockdown of CACYBP significantly hindered the progression of LUAD cells both *in vitro* and *in vivo* by reducing proliferation, enhancing apoptosis, and limiting migration and invasion. This suggests that CACYBP serves as a critical oncogenic driver in LUAD, consistent with its oncogenic role in other malignancies such as liver, prostate, pancreatic, and colon cancers as well as cholangiocarcinoma [13-15, 29, 30]. Our results identified high CACYBP expression as being associated with advanced neoplasia and poor prognosis, indicating its potential role as a predictive biomarker for identifying high-risk LUAD patients who may require aggressive treatment. Similar biomarker-driven stratification has been successfully implemented for PD-L1 in NSCLC to guide immunotherapy decisions [39]. Furthermore, our data indicate that CACYBP knockdown suppresses tumor growth both *in vitro* and *in vivo*, highlighting CACYBP as a promising therapeutic target. The development of small-molecule inhibitors or RNA interference (RNAi)-based therapies, such as siRNA or shRNA delivered via lipid nanoparticles, could be pursued to silence CACYBP, thereby blocking the synthesis of CACYBP proteins and preventing their interaction with related proteins [40, 41]. Future research should focus on developing selective and safe CACYBP inhibitors for clinical application, utilizing artificial intelligence and machine learning in computational chemistry and molecular docking to identify novel, effective inhibitors and facilitate clinical translation.

Gene expression profiling was carried out to determine the molecular mechanism by which CACYBP regulates LUAD using bioinformatic analysis, and CDK1 was found to be a candidate target of CACYBP. Subsequent validation revealed that CDK1 expression was significantly enhanced in LUAD tissues compared with normal tissues. More importantly, we proved that CDK1 coimmunoprecipitated with CACYBP in NCI-H1299 cells, indicating an

interaction between CACYBP and CDK1. Therefore, CDK1 was a downstream CACYBP target controlling NCI-H1299 cells.

CDK1 is a serine/threonine kinase family member. It functions as a pleiotropic cell cycle regulator, driving cells through the G2 phase and into mitosis by interacting with its catalytic partner, cyclin B [42]. In addition to its role in cell cycle regulation, CDK1 is a translational activator, allowing protein synthesis to adapt directly to the cell proliferation rate [43]. CDK1 could be associated with the malignant phenotype of lung cancer. For instance, higher CDK1 transcript and protein levels were observed in lung cancer samples than in normal samples. Moreover, a positive association with tumor stage indicated that elevated CDK1 expression had adverse survival outcomes [44]. CDK1 can mediate the promoting effect of NUCKS1 overexpression on the proliferation, invasion, and migration of NSCLC cells [45]. This study established the potential of CDK1 overexpression to promote the growth and motility and inhibit the apoptosis of LUAD cells. Additionally, CDK1 overexpression mitigates the inhibitory impact of CACYBP knockdown on LUAD cell development, thereby linking CDK1 to the regulation of LUAD driven by CACYBP.

Our study elucidates that CACYBP directly interacts with CDK1, as evidenced by co-IP assays. Targeting the CACYBP-CDK1 complex might be a therapeutic approach for LUAD. Although protein-protein interactions like CACYBP-CDK1 are hard to target, high-throughput screening and structure-based drug design could help find small molecules to disrupt this interaction [46, 47]. Existing pan-CDK inhibitors, such as Dinaciclib and Seliciclib, which target multiple CDKs, could be promising for LUAD, especially in tumors highly dependent on CDK1 [48]. Dinaciclib has been effective in trials for leukemia, breast, and pancreatic cancers[49-51], while Seliciclib has been tested in various cancers [52, 53]. RO-3306, a selective CDK1 inhibitor, has shown antitumor effects in studies, but its toxicity to normal cells, particularly the hematopoietic system, limits its clinical use [54-56]. Combining CDK inhibitors with other cancer treatments, such as chemotherapy or immune checkpoint inhibitors, may enhance their effectiveness [56].

In this study, IPA revealed that the PI3K/AKT signaling pathway was significant in the subsequent molecular events when NCI-H1299 cells were treated with shCACYBP. PI3K/AKT signaling is an important intracellular signal transduction pathway whose dysregulation is related to cell proliferation, invasion, autophagy, and metastasis in LUAD [57]. Importantly, activation of the PI3K/AKT pathway has previously been shown to be an

early pathogenic event in the tumorigenesis and progression of NSCLC [58, 59]. Rescue experiments showed that treatment with the PI3K inhibitor LY294002 partially reversed the CDK1 effects on promoting the proliferation and inhibiting the apoptosis of A549 and NCI-H1299 cells. This finding supports our hypothesis that CDK1 may exert a tumorigenic effect on LUAD cells partly via the PI3K/AKT pathway and implies that the pathway could be involved in CACYBP-regulated LUAD progression.

Our work has several limitations. First, we initially showed that CDK1 is involved in the process by which CACYBP knockdown inhibits the malignant progression of LUAD, but the specific binding site and the exact binding mechanism between CACYBP and CDK1 remain unknown. Second, the findings regarding the PI3K/AKT signaling pathway are preliminary, and a more detailed mechanism by which CACYBP regulates the PI3K/AKT signaling pathway via CDK1 remains to be further explored. These issues are the focus of our ongoing attention in subsequent exploration experiments (Figure S3 and S4). Despite the limitations, this study provides novel insights into the role of CACYBP and suggests that targeting CACYBP with RNAi could be a promising strategy for managing LUAD. Translational efforts should focus on developing CACYBP-directed therapies and integrating them with existing CDK1 or PI3K/AKT inhibitors to improve outcomes for advanced LUAD patients.

CONCLUSION

Our findings revealed that elevated CACYBP expression in LUAD is associated with advanced neoplasia and poor prognosis. CACYBP knockdown significantly attenuated the growth of LUAD cells. Notably, CACYBP may play a carcinogenic role in LUAD at least partly by targeting CDK1 to activate the PI3K/AKT signaling pathway. Thus, CACYBP could become a potential prognostic marker or therapeutic target in LUAD.

Conflicts of interest: Authors declare no conflicts of interest.

Funding: This study was supported by grants from Natural Science Foundation of Guangdong Province, China (2023A1515011600).

Data availability: The datasets used and/or analyzed during the current study are available from the corresponding author on reasonable request.

Submitted: 10 December 2024

Accepted: 16 March 2025

Published online: March 2025

REFERENCES

[1] Siegel RL, Miller KD, Wagle NS, Jemal A. Cancer statistics, 2023. CA Cancer J Clin 2023;73(1):17-48. https://doi.org/10.3322/caac.21763.
[2] Houston KA, Mitchell KA, King J, White A, Ryan BM. Histologic Lung Cancer Incidence Rates and Trends Vary by Race/Ethnicity and Residential County. J Thorac Oncol 2018;13(4):497-509. https://doi.org/10.1016/j.jtho.2017.12.010.
[3] Travis WD. Pathology of lung cancer. Clin Chest Med 2011;32(4):669-692. https://doi.org/10.1016/j.ccm.2011.08.005.
[4] Goebel C, Louden CL, McKenna R, Jr., Onugha O, Wachtel A, Long T. Diagnosis of Non-small Cell Lung Cancer for Early Stage Asymptomatic Patients. Cancer Genomics Proteomics 2019;16(4):229-244. https://doi.org/10.21873/cgp.20128.
[5] Simeone JC, Nordstrom BL, Patel K, Klein AB. Treatment patterns and overall survival in metastatic non-small-cell lung cancer in a real-world, US setting. Future Oncol 2019;15(30):3491-3502. https://doi.org/10.2217/fon-2019-0348.
[6] Xia L, Liu Y, Wang Y. PD-1/PD-L1 blockade therapy in advanced non-small-cell lung cancer: current status and future directions. Oncologist 2019;24(Suppl 1):S31-S41. https://doi.org/10.1634/theoncologist.2019-IO-S1-s05.
[7] Yu Y, Zeng D, Ou Q, Liu S, Li A, Chen Y, et al. Association of survival and immune-related biomarkers with immunotherapy in patients with non-small cell lung cancer: A meta-analysis and individual patient-level analysis. JAMA Netw Open 2019;2(7):e196879. https://doi.org/10.1001/jamanetworkopen.2019.6879.
[8] Hirsch FR, Scagliotti GV, Mulshine JL, Kwon R, Curran WJ, Jr., Wu YL, et al. Lung cancer: current therapies and new targeted treatments. Lancet 2017;389(10066):299-311. https://doi.org/10.1016/S0140-6736(16)30958-8.
[9] Jiang TX, Zou JB, Zhu QQ, Liu CH, Wang GF, Du TT, et al. SIP/CacyBP promotes autophagy by regulating levels of BRUCE/Apollon, which stimulates LC3-I degradation. Proc Natl Acad Sci U S A 2019;116(27):13404-13413. https://doi.org/10.1073/pnas.1901039116.
[10] Filipek A, Leśniak W. Current view on cellular function of S100A6 and its ligands, CacyBP/SIP and Sgt1. Postepy Biochem 2018;64(3):242-252. https://doi.org/10.18388/pb.2018_136.
[11] Topolska-Woś AM, Chazin WJ, Filipek A. CacyBP/SIP--Structure and variety of functions. Biochim Biophys Acta 2016;1860(1 Pt A):79-85. https://doi.org/10.1016/j.bbagen.2015.10.012.
[12] Bhattacharya S, Lee YT, Michowski W, Jastrzebska B, Filipek A, Kuznicki J, et al. The modular structure of SIP facilitates its role in stabilizing multiprotein assemblies. Biochemistry 2005;44(27):9462-9471. https://doi.org/10.1021/bi0502689.
[13] Zhang Y, Liu L, Luo B, Tang H, Yu X, Bao S. Calcyclin-binding protein contributes to cholangiocarcinoma progression by inhibiting ubiquitination of MCM2. Oncology Research 2023;31(3):317-331. https://doi.org/10.32604/or.2023.028418.
[14] Li Q, Liu Z, Ma L, Yin W, Zhang K. CACYBP knockdown inhibits progression of prostate cancer via p53. J Cancer Res Clin Oncol 2023;149(9):5761-5772. https://doi.org/10.1007/s00432-022-04497-x.
[15] Lian YF, Huang YL, Zhang YJ, Chen DM, Wang JL, Wei H, et al. CACYBP enhances cytoplasmic retention of P27(Kip1) to promote hepatocellular carcinoma progression in the absence of RNF41 mediated degradation. Theranostics 2019;9(26):8392-8408. https://doi.org/10.7150/thno.36838.
[16] Zhao W, Wang C, Wang J, Ge A, Li Y, Li W, et al. Relationship between CacyBP/SIP expression and prognosis in astrocytoma. J Clin Neurosci 2011;18(9):1240-1244. https://doi.org/10.1016/j.jocn.2011.01.024.
[17] Sun S, Ning X, Liu J, Liu L, Chen Y, Han S, et al. Overexpressed CacyBP/SIP leads to the suppression of growth in renal cell carcinoma. Biochem Biophys Res Commun 2007;356(4):864-871. https://doi.org/10.1016/j.bbrc.2007.03.080.
[18] Nie F, Yu XL, Wang XG, Tang YF, Wang LL, Ma L. Down-regulation of CacyBP is associated with poor prognosis and the effects on COX-2 expression in breast cancer. Int J Oncol 2010;37(5):1261-1269. https://doi.org/10.3892/ijo_00000777.
[19] Kilańczyk E, Gwoździński K, Wilczek E, Filipek A. Up-regulation of CacyBP/SIP during rat breast cancer development. Breast Cancer 2014;21(3):350-357. https://doi.org/10.1007/s12282-012-0399-1.
[20] Zhang P, Pei S, Gong Z, Feng Y, Zhang X, Yang F, et al. By integrating single-cell RNA-seq and bulk RNA-seq in sphingolipid metabolism, CACYBP was identified as a potential therapeutic target in lung adenocarcinoma. Front Immunol 2023;141115272. https://doi.org/10.3389/fimmu.2023.1115272.

[21] Colaprico A, Silva TC, Olsen C, Garofano L, Cava C, Garolini D, et al. TCGAbiolinks: an R/Bioconductor package for integrative analysis of TCGA data. Nucleic Acids Res 2016;44(8):e71. https://doi.org/10.1093/nar/gkv1507.
[22] Love MI, Huber W, Anders S. Moderated estimation of fold change and dispersion for RNA-seq data with DESeq2. Genome Biol 2014;15(12):550. https://doi.org/10.1186/s13059-014-0550-8.
[23] Jurmeister P, Bockmayr M, Treese C, Stein U, Lenze D, Johrens K, et al. Immunohistochemical analysis of Bcl-2, nuclear S100A4, MITF and Ki67 for risk stratification of early-stage melanoma - A combined IHC score for melanoma risk stratification. J Dtsch Dermatol Ges 2019;17(8):800-808. https://doi.org/10.1111/ddg.13917.
[24] MacArthur Clark JA, Sun D. Guidelines for the ethical review of laboratory animal welfare People's Republic of China National Standard GB/T 35892‐2018 [Issued 6 February 2018 Effective from 1 September 2018]. Animal Models and Experimental Medicine 2020;3(1):103-113. https://doi.org/10.1002/ame2.12111.
[25] Benjamini Y, Hochberg Y. Controlling the false discovery rate: A practical and powerful approach to multiple testing. Journal of the Royal Statistical Society: Series B (Methodological) 1995;57(1):289-300. https://doi.org/10.1111/j.2517-6161.1995.tb02031.x.
[26] Zhai H, Shi Y, Jin H, Li Y, Lu Y, Chen X, et al. Expression of calcyclin-binding protein/Siah-1 interacting protein in normal and malignant human tissues: an immunohistochemical survey. J Histochem Cytochem 2008;56(8):765-772. https://doi.org/10.1369/jhc.2008.950519.
[27] Chen X, Han G, Zhai H, Zhang F, Wang J, Li X, et al. Expression and clinical significance of CacyBP/SIP in pancreatic cancer. Pancreatology 2008;8(4-5):470-477. https://doi.org/10.1159/000151774.
[28] Mo B. Pan-analysis reveals CACYBP to be a novel prognostic and predictive marker for multiple cancers. American Journal of Translational Research 2024;16(1):12-26. https://doi.org/10.62347/owvw7440.
[29] Chen X, Mo P, Li X, Zheng P, Zhao L, Xue Z, et al. CacyBP/SIP protein promotes proliferation and G1/S transition of human pancreatic cancer cells. Mol Carcinog 2011;50(10):804-10. https://doi.org/10.1002/mc.20737.
[30] Zhai H, Shi Y, Chen X, Wang J, Lu Y, Zhang F, et al. CacyBP/SIP promotes the proliferation of colon cancer cells. PLoS One 2017;12(2):e0169959. https://doi.org/10.1371/journal.pone.0169959.
[31] Niu YL, Li YJ, Wang JB, Lu YY, Liu ZX, Feng SS, et al. CacyBP/SIP nuclear translocation regulates p27Kip1 stability in gastric cancer cells. World J Gastroenterol 2016;22(15):3992-4001. https://doi.org/10.3748/wjg.v22.i15.3992.
[32] Zhai HH, Meng J, Wang JB, Liu ZX, Li YF, Feng SS. CacyBP/SIP nuclear translocation induced by gastrin promotes gastric cancer cell proliferation. World J Gastroenterol 2014;20(29):10062-10070. https://doi.org/10.3748/wjg.v20.i29.10062.
[33] Chen Y, Zhang K, Wang X, Li Q, Wu Q, Ning X. Cell cycle-dependent translocation and regulatory mechanism of CacyBP/SIP in gastric cancer cells. Anticancer Drugs 2018;29(1):19-28. https://doi.org/10.1097/CAD.0000000000000556.
[34] Ning X, Sun S, Hong L, Liang J, Liu L, Han S, et al. Calcyclin-binding protein inhibits proliferation, tumorigenicity, and invasion of gastric cancer. Mol Cancer Res 2007;5(12):1254-1262. https://doi.org/10.1158/1541-7786.MCR-06-0426.
[35] Tang Y, Zhan W, Cao T, Tang T, Gao Y, Qiu Z, et al. CacyBP/SIP inhibits Doxourbicin-induced apoptosis of glioma cells due to activation of ERK1/2. IUBMB Life 2016;68(3):211-219. https://doi.org/10.1002/iub.1477.
[36] Shi H, Gao Y, Tang Y, Wu Y, Gong H, Du J, et al. CacyBP/SIP protein is important for the proliferation of human glioma cells. IUBMB Life 2014;66(4):286-291. https://doi.org/10.1002/iub.1263.
[37] Yan S, Li A, Liu Y. CacyBP/SIP inhibits the migration and invasion behaviors of glioblastoma cells through activating Siah1 mediated ubiquitination and degradation of cytoplasmic p27. Cell Biol Int 2018;42(2):216-226. https://doi.org/10.1002/cbin.10889.
[38] Wang N, Ma Q, Wang Y, Ma G, Zhai H. CacyBP/SIP expression is involved in the clinical progression of breast cancer. World J Surg 2010;34(11):2545-52. https://doi.org/10.1007/s00268-010-0690-2.
[39] Brody R, Zhang Y, Ballas M, Siddiqui MK, Gupta P, Barker C, et al. PD-L1 expression in advanced NSCLC: Insights into risk stratification and treatment selection from a systematic literature review. Lung Cancer 2017;112200-215. https://doi.org/10.1016/j.lungcan.2017.08.005.
[40] El Moukhtari SH, Garbayo E, Amundarain A, Pascual-Gil S, Carrasco-León A, Prosper F, et al. Lipid nanoparticles for siRNA delivery in cancer treatment. Journal of Controlled Release 2023;361130-146. https://doi.org/10.1016/j.jconrel.2023.07.054.
[41] Barata P, Sood AK, Hong DS. RNA-targeted therapeutics in cancer clinical trials: Current status and future directions. Cancer Treatment Reviews 2016;5035-47. https://doi.org/10.1016/j.ctrv.2016.08.004.
[42] Hochegger H, Takeda S, Hunt T. Cyclin-dependent kinases and cell-cycle transitions: does one fit all? Nat Rev Mol Cell Biol 2008;9(11):910-6. https://doi.org/10.1038/nrm2510.

[43] Haneke K, Schott J, Lindner D, Hollensen AK, Damgaard CK, Mongis C, et al. CDK1 couples proliferation with protein synthesis. J Cell Biol 2020;219(3):e201906147. https://doi.org/10.1083/jcb.201906147.
[44] Li M, He F, Zhang Z, Xiang Z, Hu D. CDK1 serves as a potential prognostic biomarker and target for lung cancer. J Int Med Res 2020;48(2):1-12. https://doi.org/10.1177/0300060519897508.
[45] Zhao S, Wang B, Ma Y, Kuang J, Liang J, Yuan Y. NUCKS1 promotes proliferation, invasion and migration of non-small cell lung cancer by upregulating CDK1 expression. Cancer Manag Res 2020;1213311-13323. https://doi.org/10.2147/CMAR.S282181.
[46] Scott DE, Bayly AR, Abell C, Skidmore J. Small molecules, big targets: drug discovery faces the protein–protein interaction challenge. Nature Reviews Drug Discovery 2016;15(8):533-550. https://doi.org/10.1038/nrd.2016.29.
[47] Sofi S, Mehraj U, Qayoom H, Aisha S, Almilaibary A, Alkhanani M, et al. Targeting cyclin-dependent kinase 1 (CDK1) in cancer: molecular docking and dynamic simulations of potential CDK1 inhibitors. Medical Oncology 2022;39(9). https://doi.org/10.1007/s12032-022-01748-2.
[48] Wang Q, Bode AM, Zhang T. Targeting CDK1 in cancer: mechanisms and implications. npj Precision Oncology 2023;7(1). https://doi.org/10.1038/s41698-023-00407-7.
[49] Flynn J, Jones J, Johnson AJ, Andritsos L, Maddocks K, Jaglowski S, et al. Dinaciclib is a novel cyclin-dependent kinase inhibitor with significant clinical activity in relapsed and refractory chronic lymphocytic leukemia. Leukemia 2015;29(7):1524-1529. https://doi.org/10.1038/leu.2015.31.
[50] Mita MM, Joy AA, Mita A, Sankhala K, Jou Y-M, Zhang D, et al. Randomized Phase II Trial of the Cyclin-Dependent Kinase Inhibitor Dinaciclib (MK-7965) Versus Capecitabine in Patients With Advanced Breast Cancer. Clinical Breast Cancer 2014;14(3):169-176. https://doi.org/10.1016/j.clbc.2013.10.016.
[51] Huang J, Chen P, Liu K, Liu J, Zhou B, Wu R, et al. CDK1/2/5 inhibition overcomes IFNG-mediated adaptive immune resistance in pancreatic cancer. Gut 2021;70(5):890-899. https://doi.org/10.1136/gutjnl-2019-320441.
[52] Cicenas J, Kalyan K, Sorokinas A, Stankunas E, Levy J, Meskinyte I, et al. Roscovitine in cancer and other diseases. Ann Transl Med 2015;3(10):135. https://doi.org/10.3978/j.issn.2305-5839.2015.03.61.
[53] Benson C, White J, Bono JD, O'Donnell A, Raynaud F, Cruickshank C, et al. A phase I trial of the selective oral cyclin-dependent kinase inhibitor seliciclib (CYC202; R-Roscovitine), administered twice daily for 7 days every 21 days. British Journal of Cancer 2006;96(1):29-37. https://doi.org/10.1038/sj.bjc.6603509.
[54] Vassilev LT, Tovar C, Chen S, Knezevic D, Zhao X, Sun H, et al. Selective small-molecule inhibitor reveals critical mitotic functions of human CDK1. Proc Natl Acad Sci U S A 2006;103(28):10660-5. https://doi.org/10.1073/pnas.0600447103.
[55] Schwermer M, Lee S, Köster J, van Maerken T, Stephan H, Eggert A, et al. Sensitivity to cdk1-inhibition is modulated by p53 status in preclinical models of embryonal tumors. Oncotarget 2015;6(17):15425-35. https://doi.org/10.18632/oncotarget.3908.
[56] Wu CX, Wang XQ, Chok SH, Man K, Tsang SHY, Chan ACY, et al. Blocking CDK1/PDK1/β-Catenin signaling by CDK1 inhibitor RO3306 increased the efficacy of sorafenib treatment by targeting cancer stem cells in a preclinical model of hepatocellular carcinoma. Theranostics 2018;8(14):3737-3750. https://doi.org/10.7150/thno.25487.
[57] Yip PY. Phosphatidylinositol 3-kinase-AKT-mammalian target of rapamycin (PI3K-Akt-mTOR) signaling pathway in non-small cell lung cancer. Transl Lung Cancer Res 2015;4(2):165-76. https://doi.org/10.3978/j.issn.2218-6751.2015.01.04.
[58] Gustafson AM, Soldi R, Anderlind C, Scholand MB, Qian J, Zhang X, et al. Airway PI3K pathway activation is an early and reversible event in lung cancer development. Sci Transl Med 2010;2(26):26ra25. https://doi.org/10.1126/scitranslmed.3000251.
[59] Massion PP, Taflan PM, Shyr Y, Rahman SM, Yildiz P, Shakthour B, et al. Early involvement of the phosphatidylinositol 3-kinase/Akt pathway in lung cancer progression. Am J Respir Crit Care Med 2004;170(10):1088-94. https://doi.org/10.1164/rccm.200404-487OC.

TABLES AND FIGURES WITH LEGENDS

Table 1. Analysis of CACYBP expression and clinicopathological characteristics in LUAD patients from TCGA dataset

Characteristics	No. of patients	CACYBP expression		*p* value
		Low	High	
All patients	490	244	246	
Age (years)				0.174
< 62	236	110	126	
≥ 62	254	134	120	
Sex				0.014
Male	226	99	127	
Female	264	145	119	
TNM stage				0.033
I	265	141	124	
II	121	60	61	
III	81	38	43	
IV	23	5	18	

CACYBP: Calcyclin-binding protein; LUAD: Lung adenocarcinoma; TCGA: The Cancer Genome Atlas.

Table 2. Analysis of CACYBP expression and clinicopathological characteristics in LUAD patients

Characteristics	No. of patients	CACYBP expression		*p* value
		Low	High	
All patients	96	52	44	
Age (years)				0.682
< 62	48	27	21	
≥ 62	48	25	23	

Sex				0.409
Male	68	35	33	
Female	28	17	11	
Tumor size (cm)				0.079
< 3.5	42	27	15	
≥ 3.5	54	25	29	
Grade				0.772
1	17	8	9	
2	55	30	25	
3	24	14	10	
TNM stage				0.041
I	35	25	10	
II	24	13	11	
III	31	12	19	
IV	6	2	4	

CACYBP: Calcyclin-binding protein; LUAD: Lung adenocarcinoma.

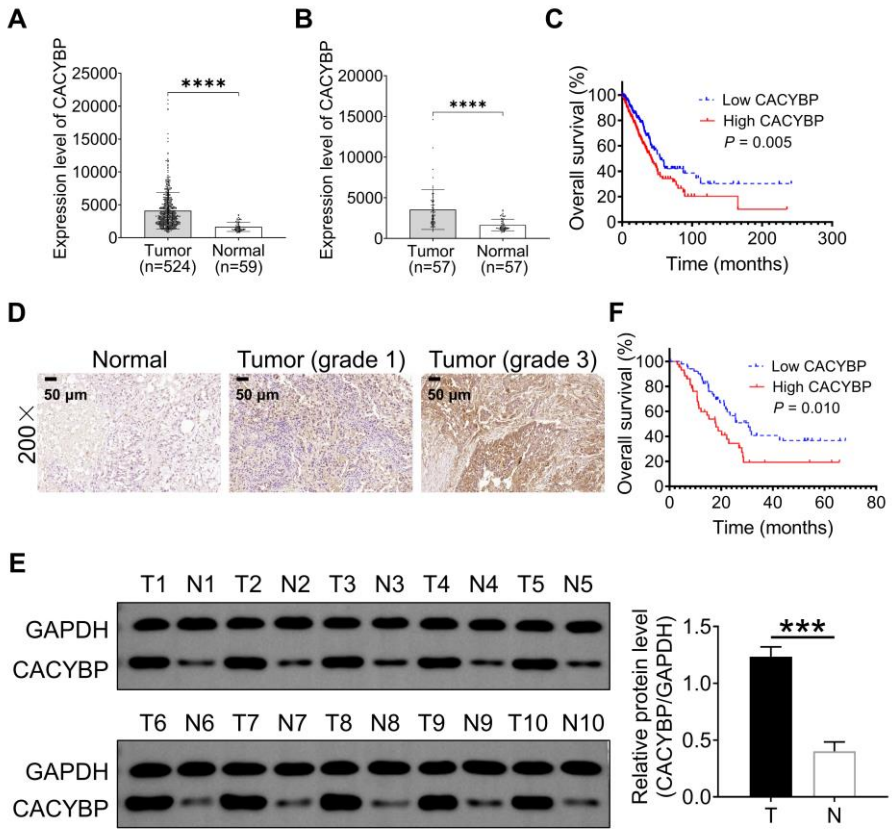

Figure 1. CACYBP expression is up-regulated in LUAD and correlated with a poor prognosis. (A and B) The distribution of CACYBP gene expression in LUAD tissue and normal tissue in the TCGA dataset, in which each point represents a sample, (A) population samples, (B) paired samples; (C) Overall survival curves predict a worse prognosis in LUAD patients with high CACYBP expression in the TCGA dataset; (D) The representative immunohistochemical CACYBP expression images of LUAD patients in adjacent normal and tumor tissues; (E) Western blotting was used to detect the expression of CACYBP in LUAD tumor tissues (T, n = 10) and adjacent normal tissues (N, n = 10); (F) Comparison of overall survival in LUAD patients with different levels of CACYBP expression. Data are shown as the mean ± SD and analyzed by paired Student's *t* test. ***$p < 0.001$ and ****$p < 0.0001$. CACYBP: Calcyclin-binding protein; LUAD: lung adenocarcinoma; TCGA: The Cancer Genome Atlas.

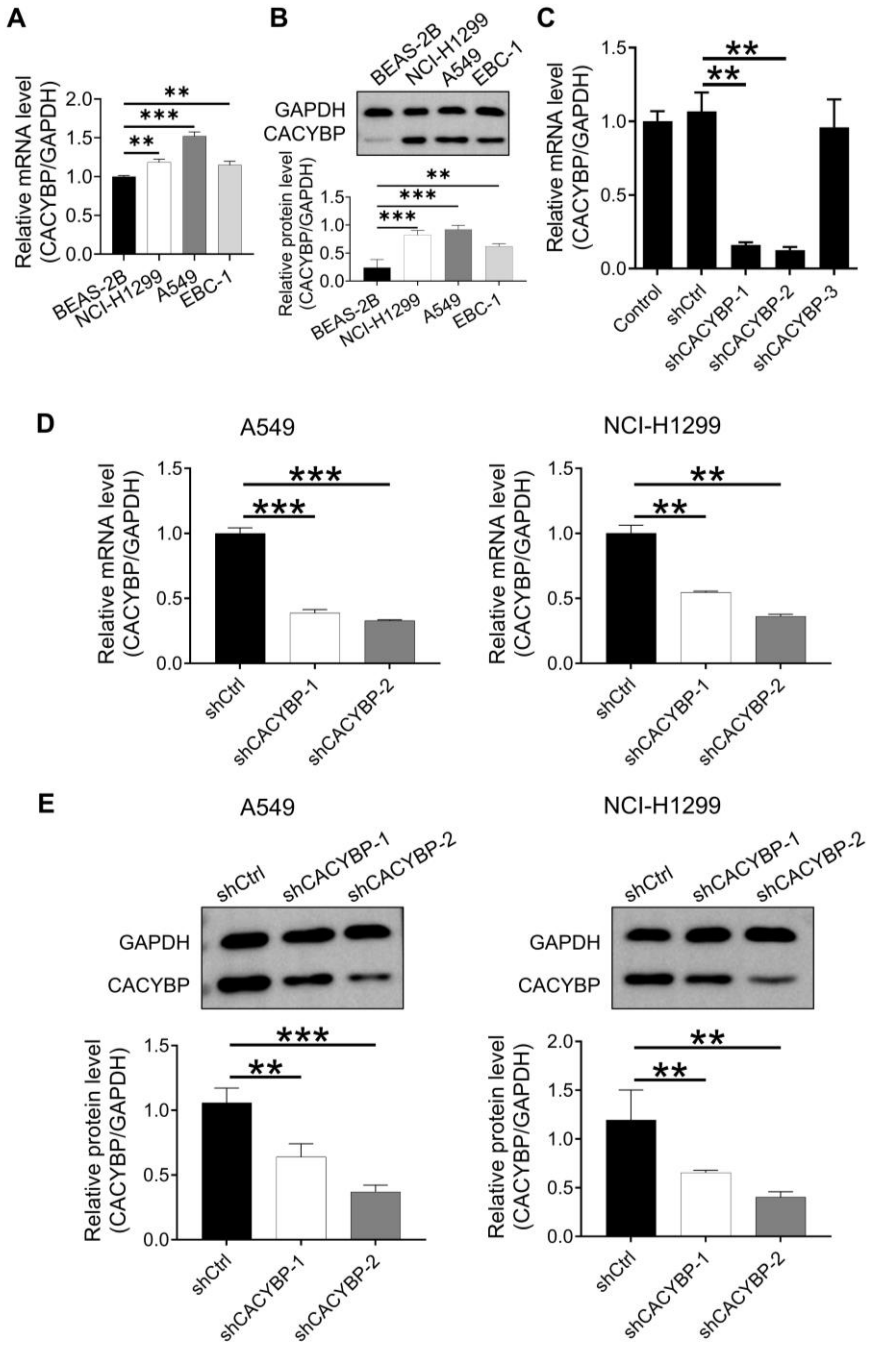

Figure 2. Development of lung cancer cell lines with CACYBP knockdown. (A and B) qRT–PCR and western blotting were used to detect the expression of CACYBP in the BEAS-2B, NCI-H1299, A549, and EBC-1 cell lines; (C) Using qRT–PCR, CACYBP knockdown effectiveness was assessed in NCI-H1299 cells; (D) qRT–PCR analysis of CACYBP expression in A549 and NCI-H1299 cell lines after transfection; (E) CACYBP protein expression in the A549 and NCI-H1299 cell lines was detected by western blotting after

transfection. All data are shown as the mean ± SD (n = 3) and analyzed by unpaired Student's *t* test. $^{**}p < 0.01$, $^{***}p < 0.001$. CACYBP: Calcyclin-binding protein; qRT–PCR: Quantitative reverse transcription polymerase chain reaction.

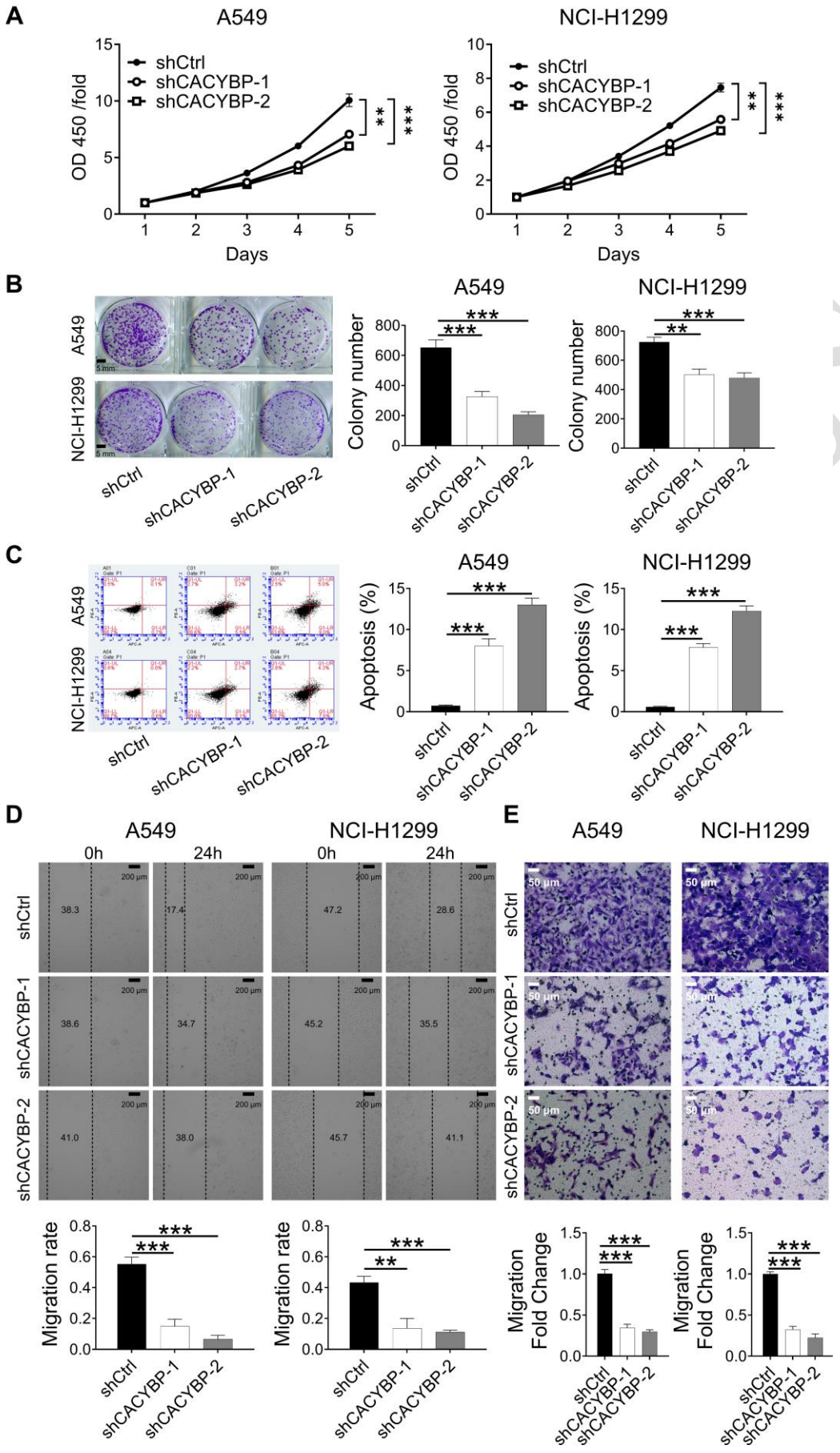
A
A549
NCI-H1299
shCtrl
shCACYBP-1
shCACYBP-2
OD 450 /fold
Days
B
Colony number
C
Apoptosis (%)
D
0h
24h
Migration rate
E
Migration Fold Change

Figure 3. CACYBP knockdown restricted LUAD cell progression *in vitro*. (A and B) CCK-8 and colony formation assays indicated the effects of CACYBP knockdown on A549 and NCI-H1299 cell proliferation; (C) The effects of CACYBP knockdown on cell apoptosis were evaluated using flow cytometry; (D and E) The effects of CACYBP knockdown on the migratory capability of A549 and NCI-H1299 cells were assessed using wound healing assays (magnification: ×50) and Transwell assays (magnification: ×200). All data are shown as the mean ± SD (n = 3) and analyzed by unpaired Student's *t* test. $^{**}p < 0.01$, $^{***}p < 0.001$. CACYBP: Calcyclin-binding protein; LUAD: lung adenocarcinoma; CCK-8: Cell counting kit-8.

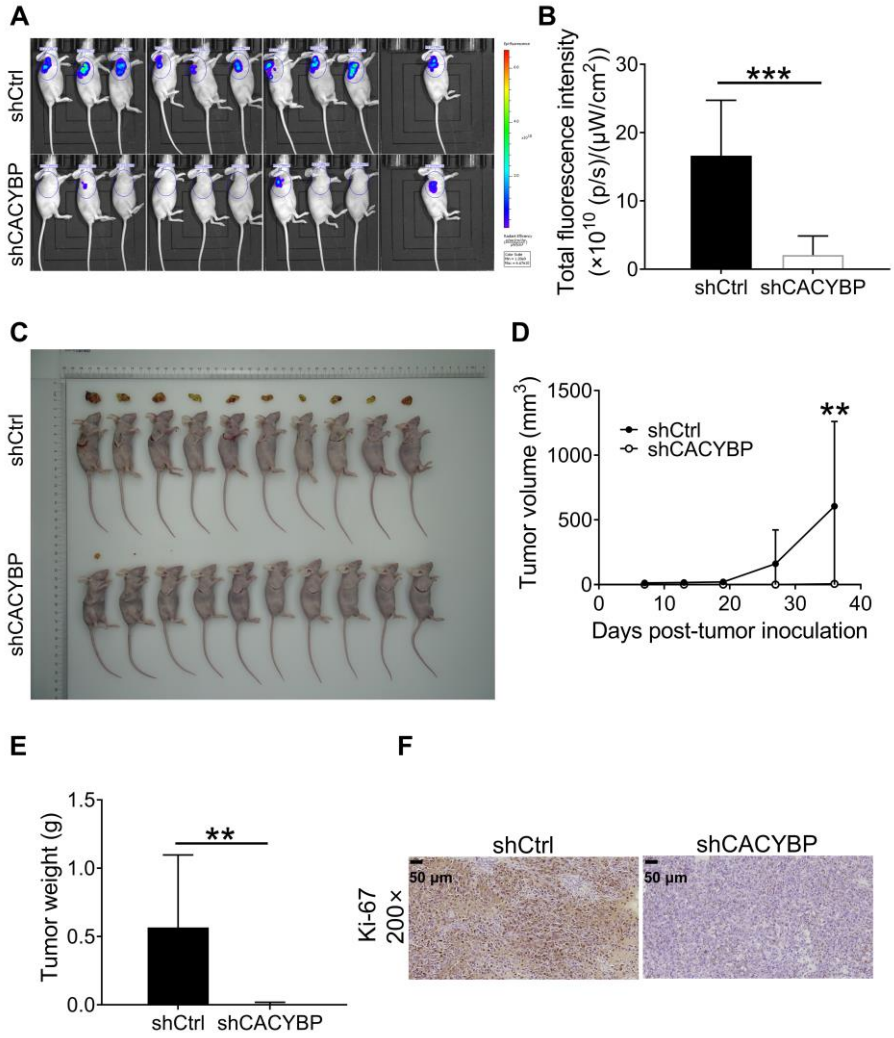

Figure 4. CACYBP knockdown restricts NCI-H1299 cell growth *in vivo*. (A) *In vivo* imaging was used to evaluate the tumor burden in the shCtrl and shCACYBP groups prior to euthanasia of mice; (B) Total fluorescence tumor intensity in both groups; (C) Photograph of resected xenograft tumors from mice in both groups; (D) Tumor volumes in both groups were determined during the experiment; (E) Tumor weight in both groups was measured after euthanasia of mice; (F) Evaluation of the Ki-67 index in resected tumors using IHC staining. $^{**}p < 0.01$, $^{***}p < 0.001$. CACYBP: Calcyclin-binding protein; IHC: Immunohistochemistry.

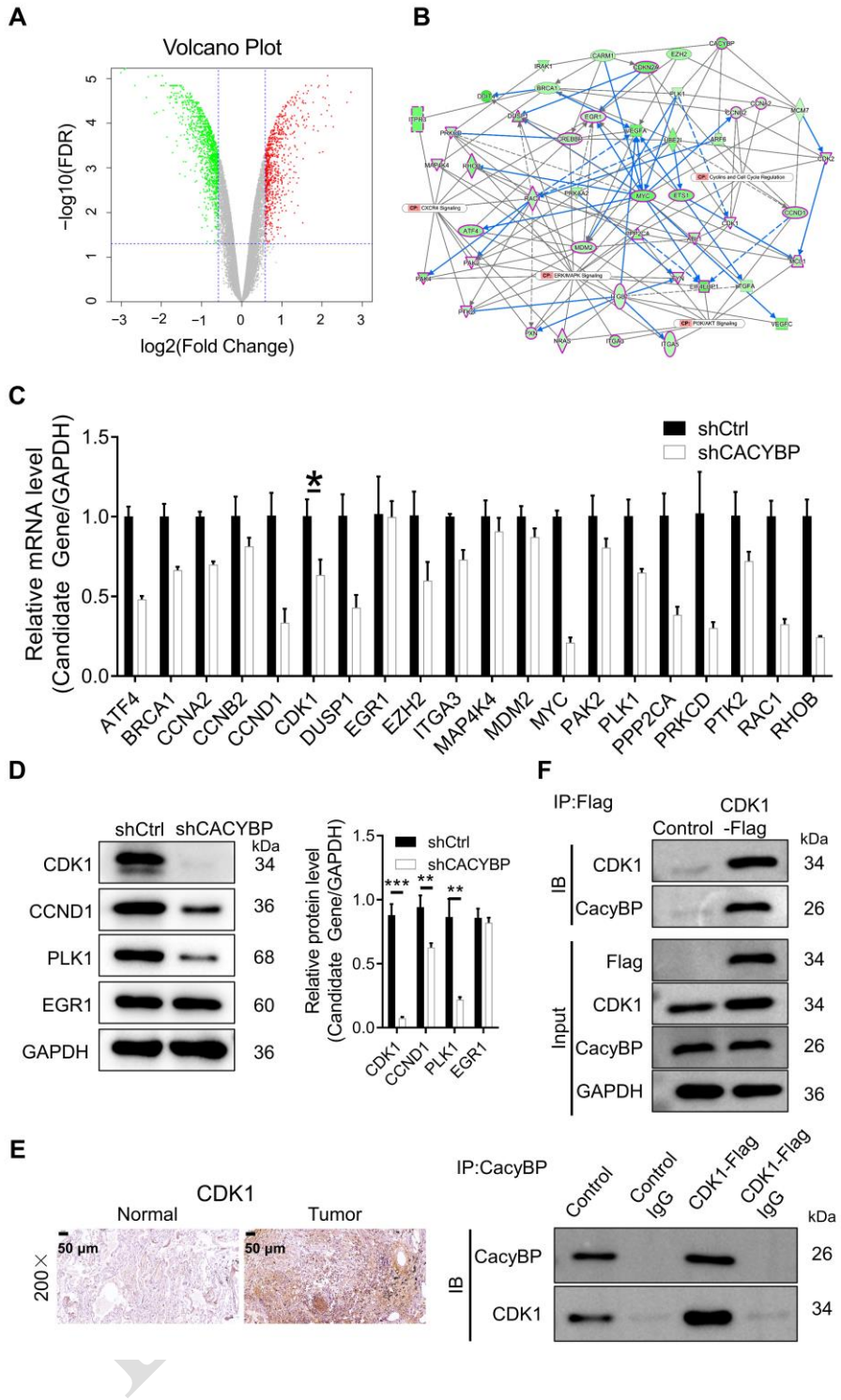

Figure 5. Exploring the downstream CACYBP mechanism in NCI-H1299 cells. (A) Volcano plot of DEGs between the experimental (shCACYBP) and control (shCtrl) groups in NCI-H1299 cells, red dots represent up-regulated genes, green dots represent down-regulated genes, and gray dots represent genes with no significant difference; (B) Interaction network between CACYBP-associated DEGs established using IPA; (C and D) The expression of

several candidate genes was examined using qRT–PCR and western blotting in NCI-H1299 cells transfected with or without shCACYBP, data are shown as the mean ± SD (n = 3) and analyzed by unpaired Student's *t* test; (E) CDK1 expression was determined in LUAD tissues and normal tissues using IHC staining; (F) A co-IP assay was used to validate the CDK1 and CACYBP interaction; Control: NCI-H1299 cells were transfected using an empty vector; CDK1-Flag: NCI-H1299 cells transfected with FLAG-tagged CDK1-overexpressing lentivirus. *$p < 0.05$, **$p < 0.01$, ***$p < 0.001$. FDR: False discovery rate; CACYBP: Calcyclin-binding protein; CDK1: Cyclin dependent kinase 1; DEGs: Differentially expressed genes; IPA: Ingenuity pathway analysis; LUAD: Lung adenocarcinoma; IHC: Immunohistochemistry; IP: Immunoprecipitation.

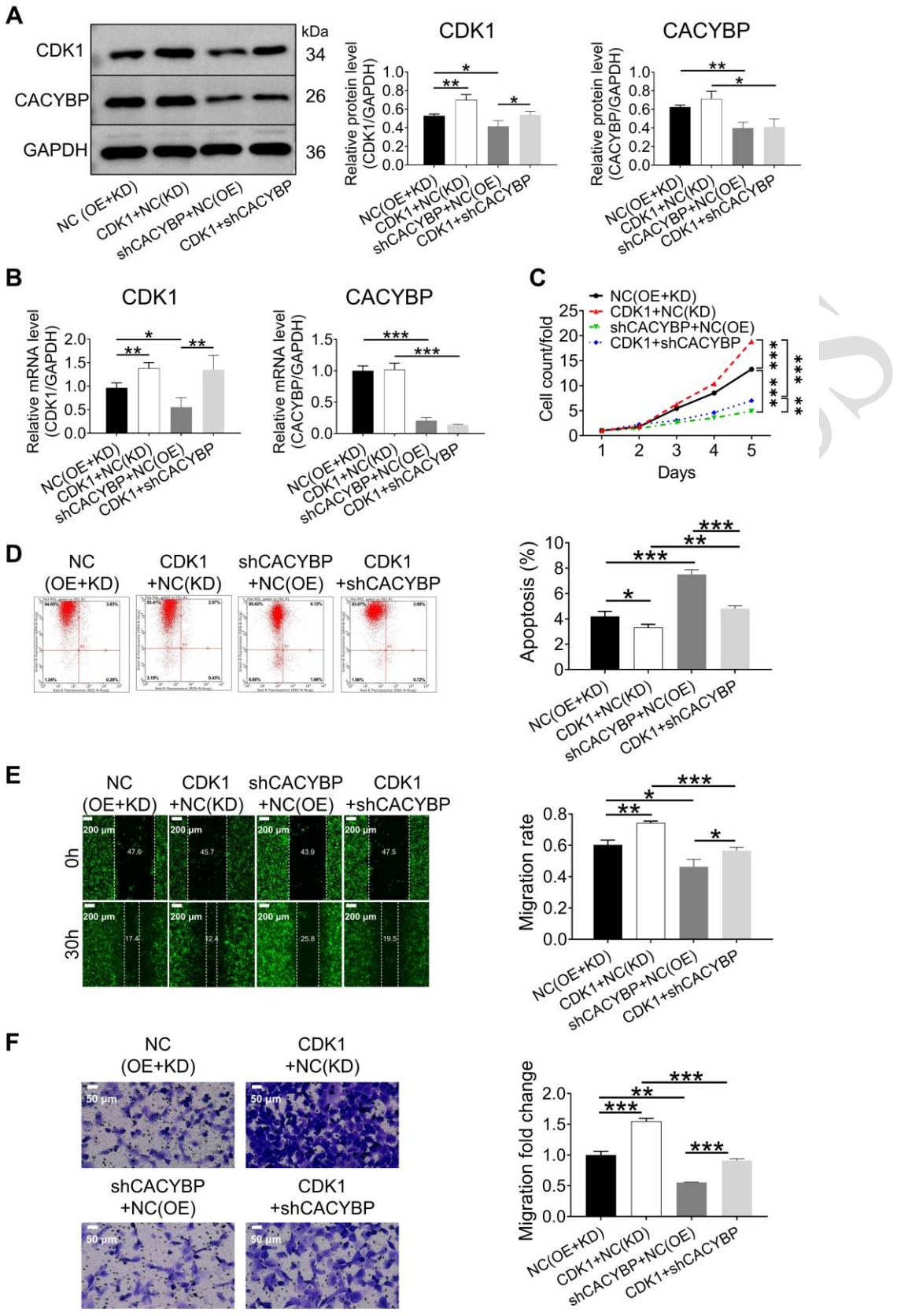
A
CDK1
CACYBP
GAPDH
kDa
34
26
36
NC (OE+KD)
CDK1+NC(KD)
shCACYBP+NC(OE)
CDK1+shCACYBP
CDK1
CACYBP
Relative protein level (CDK1/GAPDH)
Relative protein level (CACYBP/GAPDH)
B
Relative mRNA level (CDK1/GAPDH)
Relative mRNA level (CACYBP/GAPDH)
C
NC(OE+KD)
CDK1+NC(KD)
shCACYBP+NC(OE)
CDK1+shCACYBP
Cell count/fold
Days
D
NC (OE+KD)
CDK1 +NC(KD)
shCACYBP +NC(OE)
CDK1 +shCACYBP
Apoptosis (%)
E
0h
30h
Migration rate
F
Migration fold change

Figure 6. CDK1 overexpression prevented the inhibitory effects of CACYBP knockdown on NCI-H1299 cells. (A and B) Western blotting and qRT–PCR were used to detect the expression of CDK1 and CACYBP in NCI-H1299 cell models; (C) Cell proliferation was assessed using the Celigo cell counting assay; (D) Flow cytometry was used to determine cell apoptosis; (E and F) Wound healing (employing GFP as reporter gene, magnification: ×50) and Transwell (magnification: ×200) tests were used to measure the capacity of cells to migrate. All data are shown as the mean ± SD (n = 3) and analyzed by one-way ANOVA. *$p < 0.05$, **$p < 0.01$, ***$p < 0.001$. CACYBP: Calcyclin-binding protein; CDK1: Cyclin dependent kinase 1; GFP: Green fluorescent protein; ANOVA: Analysis of variance.

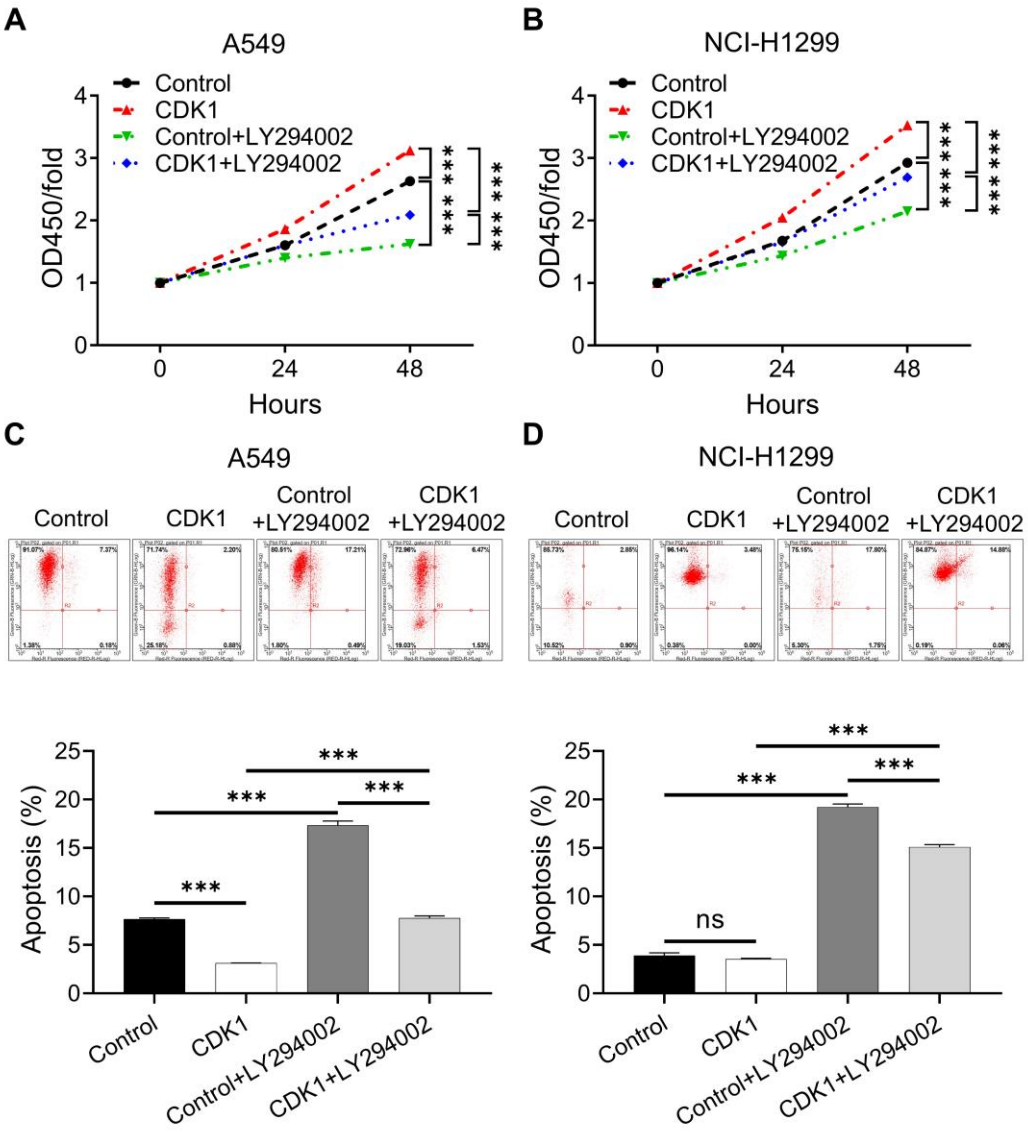
A
A549
Control
CDK1
Control+LY294002
CDK1+LY294002
OD450/fold
Hours
B
NCI-H1299
C
A549
Control
CDK1
Control +LY294002
CDK1 +LY294002
D
NCI-H1299
Apoptosis (%)
ns

Figure 7. The effects of CDK1 on LUAD cell growth were carried out via the PI3K/AKT pathway. Following a 24-hour treatment with LY294002 (50 μM), (A and B) Cell proliferation and (C and D) cell apoptosis were measured using the CCK-8 assay and flow cytometry, respectively. All data are shown as the mean ± SD (n = 3) and analyzed by one-way ANOVA. ns: no significance, ***$p < 0.001$. OD: Optical density; CDK1: Cyclin dependent kinase 1; LUAD: Lung adenocarcinoma; PI3K: Phosphatidylinositol 3-kinase; AKT: Protein kinase B; CCK-8: Cell counting kit-8; ANOVA: Analysis of variance.

SUPPLEMENTAL DATA

Supplemental data are available at the following link: